

pubs.acs.org/JPCL Letter

# Size-Dependent Onset of Nitric Acid Dissociation in $Cs^+ \cdot (HNO_3)(H_2O)_{n=0-11}$ Clusters at 20 K

Sayoni Mitra, Nan Yang, Laura M. McCaslin, R. Benny Gerber, and Mark A. Johnson\*



Cite This: J. Phys. Chem. Lett. 2021, 12, 3335-3342



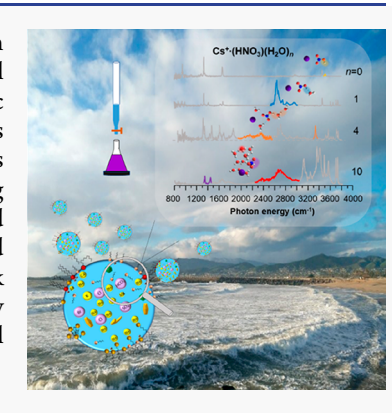
**ACCESS** 

Metrics & More



Supporting Information

**ABSTRACT:** We report the water-mediated charge separation of nitric acid upon incorporation into size-selected  $Cs^+\cdot(HNO_3)(H_2O)_{n=0-11}$  clusters at 20 K. Dramatic spectral changes are observed in the n=7-9 range that are traced to the formation of many isomeric structures associated with intermediate transfer of the acidic proton to the water network. This transfer is complete by n=10, which exhibits much simpler vibrational band patterns consistent with those expected for a tricoordinated hydronium ion (the Eigen motif) along with the NO stretching bands predicted for a hydrated  $NO_3^-$  anion that is directly complexed to the  $Cs^+$  cation. Theoretical analysis of the n=10 spectrum indicates that the dissociated ions adopt a solvent-separated ion-pair configuration such that the  $Cs^+$  and  $Cs^+$  cations flank the  $Cs^-$  anion in a microhydrated salt bridge. This charge separation motif is evidently assisted by the electrostatic stabilization of the product  $NO_3^-/H_3O^+$  ion pair by the proximal metal ion.



Titric acid plays a fundamental role in the interfacial chemistry of aerosol particles, 1-7 which in turn depends on the speciation of HNO3 in the reduced hydration environment available at or near the surface. Understanding these processes at the molecular level has motivated recent efforts to establish the acidity  $(pK_a)$  of HNO<sub>3</sub> at an interface, which is surprisingly complex. For example, despite the fact that HNO<sub>3</sub> is a strong acid in aqueous solution (p $K_a = -1.4$ ), there are many studies reporting that it is largely undissociated at the interface with neat water, although the degree of suppression has been difficult to quantify. 8-21 To access how ions affect the acidity of HNO3, Mishra et al.<sup>22</sup> calculated the structures of Cl<sup>-</sup>·(H<sub>2</sub>O)<sub>20</sub> clusters with an HNO<sub>3</sub> molecule incorporated into them and concluded that the electrostatic interaction of the dissociated ion pair with the nearby anion (Cl<sup>-</sup>) enhances HNO<sub>3</sub> dissociation. On the experimental side, Castleman and co-workers<sup>23</sup> interpreted the size-dependent HNO<sub>3</sub> uptake displayed by  $M^+ \cdot (H_2O)_{n=0-30}$  (M = Na<sup>+</sup>, K<sup>+</sup>, H<sub>3</sub>O<sup>+</sup>) clusters to indicate that acid dissociation was occurring in all systems with an onset at n = 4-5. In this Letter, we use cryogenic ion vibrational spectroscopy<sup>24</sup> to establish the structural transformations that occur when HNO3 is attached to  $Cs^+ \cdot (H_2O)_{n=0-11}$  clusters. This information is obtained by analyzing the evolution of the vibrational band patterns arising from HNO<sub>3</sub> and its conjugate base (NO<sub>3</sub><sup>-</sup>), as well as those derived from the water network as water molecules are sequentially added to the Cs<sup>+</sup>·(HNO<sub>3</sub>) binary complex.

This study extends an earlier report<sup>25</sup> that quantified the intramolecular distortions suffered by the HNO<sub>3</sub> molecule in the Cs<sup>+</sup>·(HNO<sub>3</sub>)(H<sub>2</sub>O)<sub>n=0-2</sub> series. That study found that the 450 cm<sup>-1</sup> red shift in the acidic OH stretch fundamental of the

bare nitric acid HNO<sub>3</sub> (bare  $\nu_{OH}^a$  in Figure 1A) upon formation of the neutral HNO<sub>3</sub>(H<sub>2</sub>O) van der Waals complex<sup>26</sup> is further displaced by 459 cm<sup>-1</sup> when the Cs<sup>+</sup> cation binds to the acid's -NO₂ group to form the ternary Cs<sup>+</sup>·(HNO₃)H₂O cationic cluster. This sandwich motif occurs in one of the two isomers adopted by the n = 1 system. The oscillator strength derived from the water-bound OH group of the acid (hereafter denoted OH<sup>a</sup>), appears as a very intense envelope ( $\nu_{OH}^{a-w}$  in Figure 1B) with a progression in soft mode combination bands (blue in Figure 1B above the OH stretching fundamental at 2641 cm<sup>-1</sup>). In that paper,<sup>25</sup> it was noted that the addition of a second water molecule retains this ternary sandwich structure as the second water adopts a position in the first hydration shell of the Cs<sup>+</sup> ion. Here we follow the structural evolution of the acid during sequential hydration in the series Cs+.  $HNO_3(H_2O)_{n=3-11}$ , which explores the size range through completion of the first hydration shell around Cs+. These structures are deduced by analysis of IR photodissociation (IRPD) spectra of the D2-tagged cluster ions cooled between 10 and 20 K.<sup>24</sup> This is accomplished using a cryogenic ion photofragmentation mass spectrometer described in the earlier paper reporting the spectra of the n = 0-2 clusters and detailed in the Supporting Information. Because the band patterns of HNO<sub>3</sub> and NO<sub>3</sub> are quite distinct, as are those associated

Received: January 22, 2021 Accepted: March 15, 2021 Published: March 29, 2021





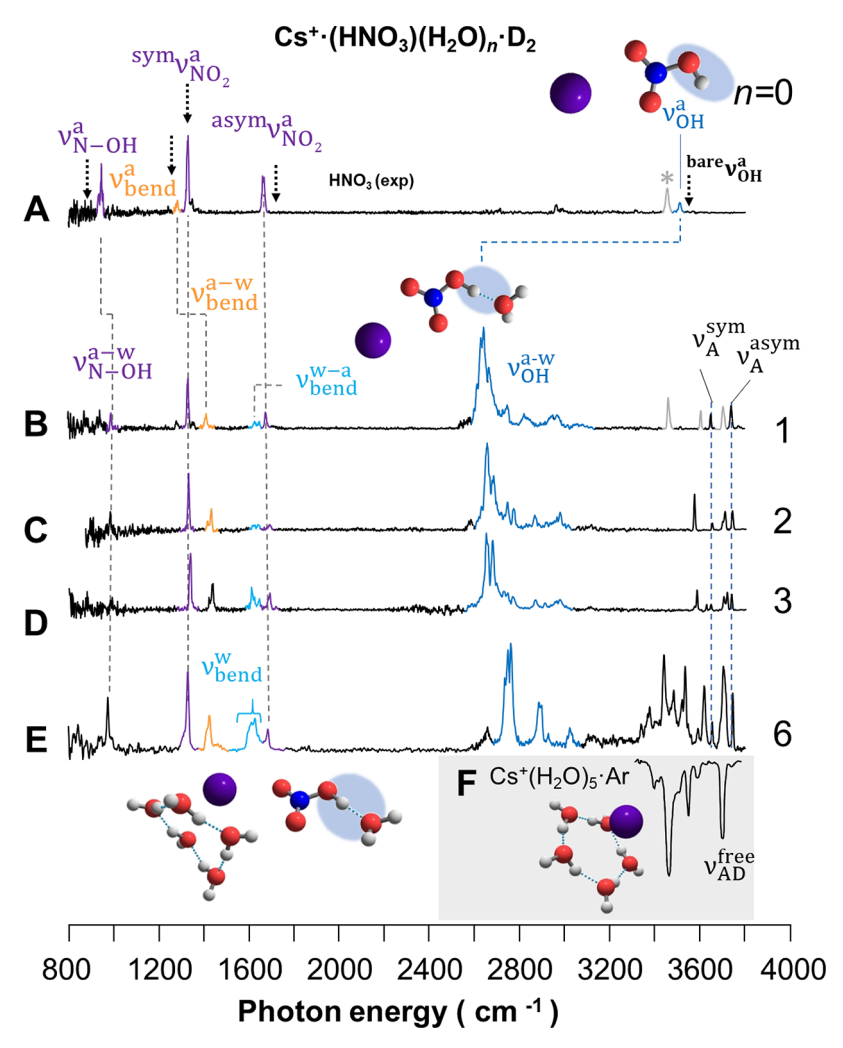


Figure 1. Survey of the isomer class corresponding to completion of the first hydration shell around Cs<sup>+</sup> with retention of the single water molecule attached to the acidic OH group of HNO<sub>3</sub>. The D<sub>2</sub>-tagged predissociation spectra of Cs<sup>+</sup>·(HNO<sub>3</sub>)(H<sub>2</sub>O)<sub>n</sub>, with n = 0, 1, 2, 3, and 6, are shown in traces A–E. The bands arising from water OH stretching modes are denoted as  $\nu_{A}^{SY}$  and  $\nu_{A}^{asym}$ , where 'A' and 'D' denote H-bond acceptor and donor configurations, while  $\nu_{bend}^{w}$  and  $\nu_{bend}^{w-a}$  indicate all transitions arising from the HOH intramolecular bending fundamental. The OH stretches from the HNO<sub>3</sub> moiety are indicated as  $\nu_{OH}^{a}$  and  $\nu_{DH}^{a-w}$ , where "a-w" indicates acid OH bound to water. The four remaining bands labeled are NO stretches; <sup>sym</sup> $\nu_{NO_2}^{a}$  and  $\nu_{NO_2}^{a-w}$  correspond to the symmetric and asymmetric normal modes of the NO<sub>2</sub> moiety, while  $\nu_{N-OH}^{a}$  and  $\nu_{N-OH}^{a-w}$  indicate the N-OH stretch of HNO<sub>3</sub>. Labels  $\nu_{bend}^{a}$  and  $\nu_{bend}^{a-w}$  indicate acidic OH bending of the free and water-bound OH groups. Arrows in A indicate key bands of the isolated HNO<sub>3</sub> molecule. <sup>4+</sup> The gray peak labeled with "\*" in A corresponds to the acid OH stretch when bound to the D<sub>2</sub> tag ( $\nu_{A}^{a-D_2}$ ). All band labels aid referencing in the text and in Tables S1 and S2. The inverted spectrum of Cs<sup>+</sup>·(H<sub>2</sub>O)<sub>5</sub>·Ar is reprinted with permission from ref 30 in trace F, along with the structure computed using B3LYP/aug-cc-pVDZ level of theory and basis set, with LANL2DZ pseudopotential used for Cs atom.

with "excess" proton accommodation by neutral water, <sup>27,28</sup> we are specifically concerned with the correlations between changes in the band patterns associated with the NO stretching fundamentals of the NO<sub>3</sub> moiety and those in the OH stretching region as reporters for the onset of intracluster dissociation of the acid into ion pairs.

We first consider the class of clusters in which the ternary "sandwich" motif reported earlier (inset in Figure 1B) is retained while the first hydration shell around the Cs<sup>+</sup> cation is completed at  $n=6.^{29}$  The traces in Figure 1B–E present the spectra of the n=1-3 and 6 clusters, for which the  $\nu_{\rm OH}^{a-w}$  band is the only feature associated with the acidic OH stretch H-bonded to a water molecule. Interestingly, the spectral pattern arising from this arrangement is most clearly articulated in the n=6 spectrum (Figure 1E), which is reproduced by the calculated (scaled) harmonic spectrum (Figure S1D(ii)), based

on the structure shown in Figure 1E. This isomer is calculated to lie 0.2 kcal/mol above the global minimum identified in Figures S1 and S2D(iii) and is consistent with the observed intact band pattern of the Cs+·(HNO<sub>3</sub>)(H<sub>2</sub>O) motif, in contrast to that of the global minimum which features strongly red-shifted OH stretching bands in the ~1800-2400 cm<sup>-1</sup> region and significantly perturbed NO stretching fundamentals. The structure in Figure 1E features a cyclic water pentamer attached to the Cs<sup>+</sup> ion, a motif adopted by the Cs<sup>+</sup>· (H<sub>2</sub>O)<sub>5</sub> cluster (Figure 1F).<sup>30,31</sup> Note that the spectral signature of the water bound to the acid OH group, which occurs in a single H-bond acceptor, or "A" configuration, yields the persistent sharp bands associated with the symmetric and antisymmetric stretches of the acceptor water molecule, indicated by the dotted lines denoted  $\nu_A^{\text{sym}}$  and  $\nu_A^{\text{asym}}$  in Figure 1B. It is also apparent that hydration directly to Cs<sup>+</sup> in the first

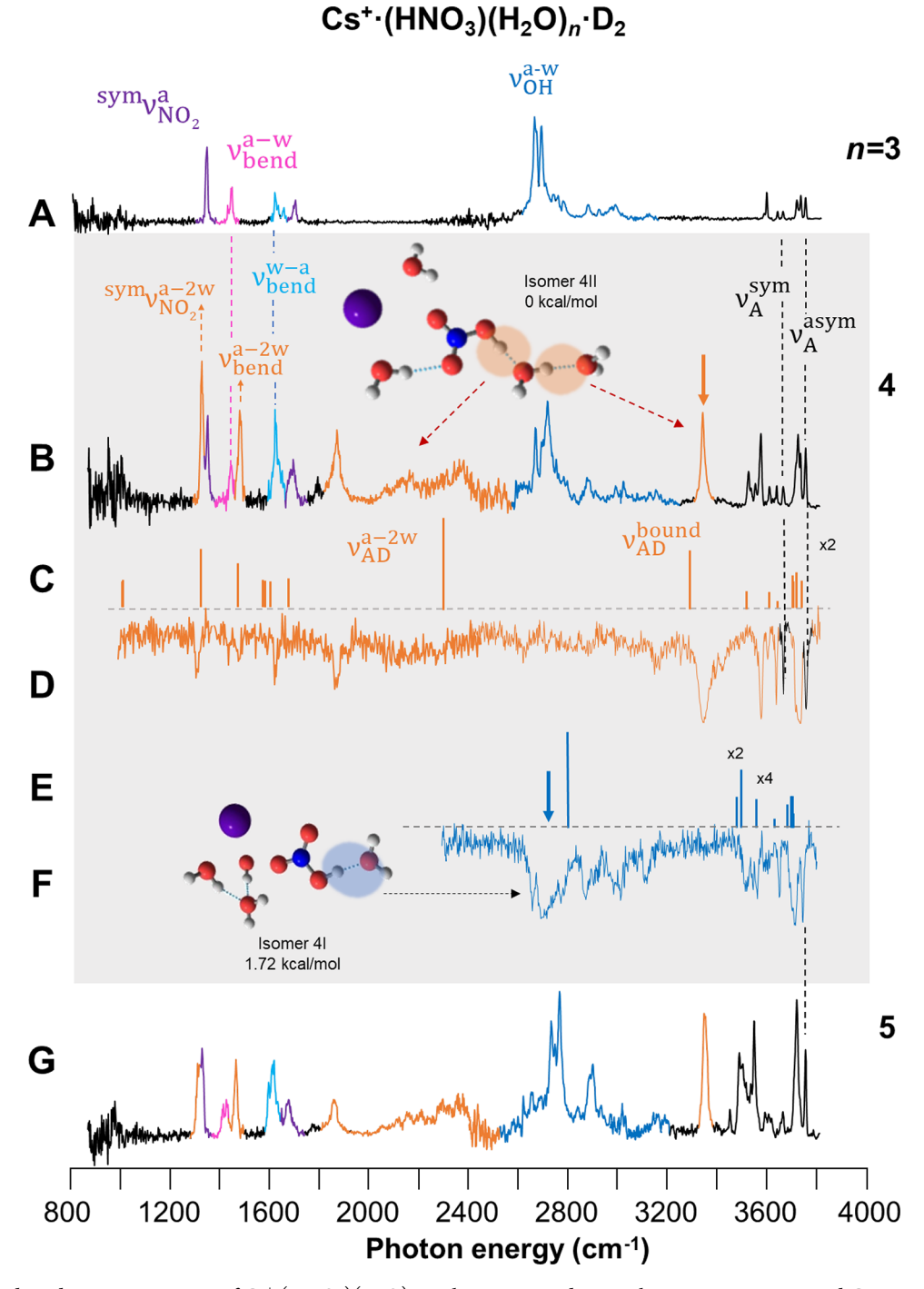


Figure 2.  $D_2$ -tagged predissociation spectra of  $Cs^+$ ·(HNO<sub>3</sub>)( $H_2O$ )<sub>n</sub>, with n = 3, 4, and 5, are shown in traces A, B, and G, respectively. In traces D and F, isomer-specific spectra of  $Cs^+$ ·(HNO<sub>3</sub>)( $H_2O$ )<sub>4</sub>· $D_2$  cluster are obtained using two-color, IR–IR double resonance by probing at the positions indicated by vertical arrows (orange, 3330 cm<sup>-1</sup> and blue, 2700 cm<sup>-1</sup>), with the corresponding isomer structures inset. The calculated spectra for isomers 4I and 4II are plotted in panels E and C, respectively. Peak labeled  $\nu_{AD}^{bound}$  corresponds to the water OH stretch H-bonded to both acid OH and second-shell water. The acid bands  $v_{NO_2}^{a-2w}$ ,  $v_{bend}^{a-2w}$  arise from attachment of the water dimer. Remaining labels are described in Figure 1 caption. All band labels aid referencing in the text and in Tables S1, S2 and S4.

solvation shell of the ion yields a solvatochromic blue shift in the acid OH stretch (by  $\sim 100~\rm cm^{-1}$  from n=1 to 6). Such blue shifts have been traced to the reduction in the local electric field for all members in the first solvation shell as new solvent dipoles are added to complete it.<sup>32</sup>

Lower in energy, the NO stretching bands of the  $HNO_3$  molecule (purple in Figure 1A) are largely intact for this series. The most pronounced effect is the  $\sim 50~{\rm cm}^{-1}$  blue shift in the

N–OH stretch (going from  $\nu_{\rm N-OH}^a$  to  $\nu_{\rm N-OH}^{a-{
m W}}$  in Figure 1A,B) upon addition of the water molecule to the acid OH group. This is accompanied by the  $\sim$ 120 cm<sup>-1</sup> blue shift in the acid OH bending mode (orange), between the  $\nu_{\rm bend}^a$  and  $\nu_{\rm bend}^{a-{
m W}}$  transitions in Figure 1A,B, falling at 1411 cm<sup>-1</sup> in the ternary motif. Finally, the water HOH bending fundamentals grow in intensity with increasing hydration to yield the broad feature (turquoise,  $\nu_{\rm bend}^{\rm W}$ ) near  $\sim$ 1630 cm<sup>-1</sup>.

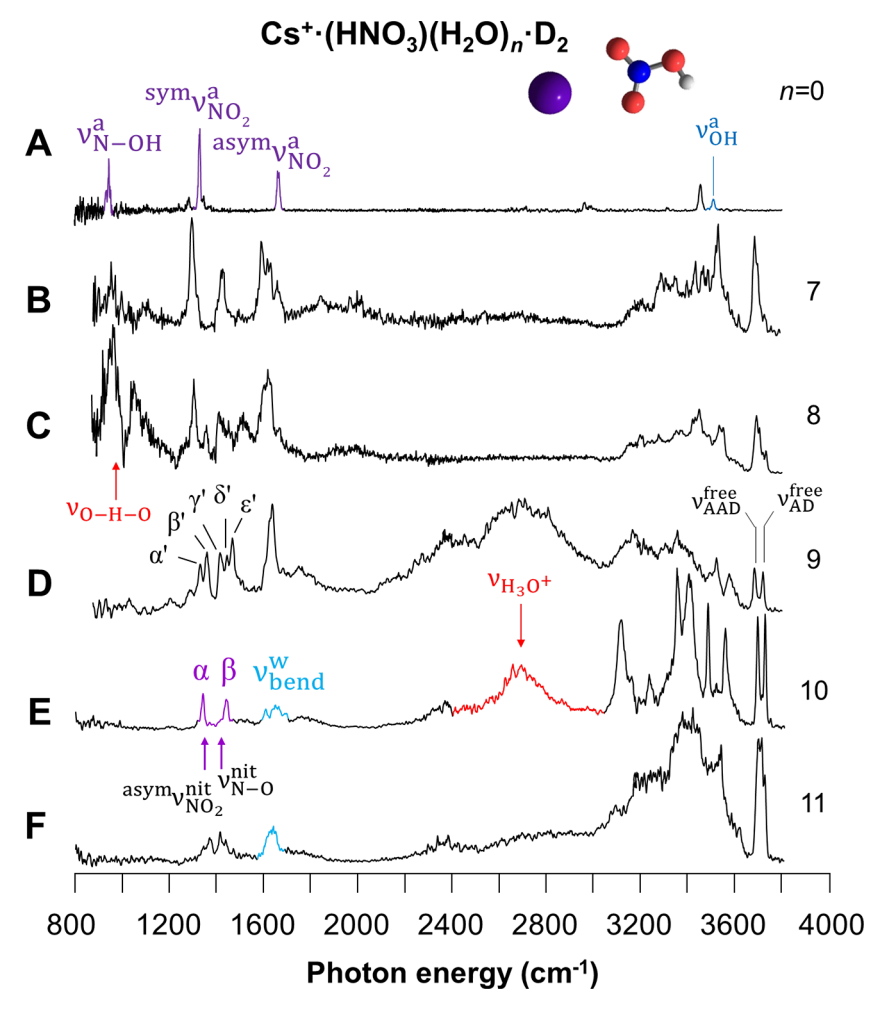


Figure 3. Vibrational predissociation spectra of  $Cs^+$ ·(HNO<sub>3</sub>)(H<sub>2</sub>O)<sub>n</sub>·D<sub>2</sub> are presented in traces A–F for n=0, 7–11. Peaks in different colors highlight specific motifs of interest. Peak labeled  $\nu_{O-H-O}$  in trace C denotes parallel stretch of equally shared bridging proton, while the red envelope ( $\nu_{H_3O^+}$ ) in E is a signature for an eigen-like motif in a cluster. The experimental bands α and β in trace E correspond to the calculated NO stretches (labeled arrows  $^{asym}\nu_{NO_2}^{nit}$  and  $\nu_{N-O}^{nit}$ , denoting NO<sub>2</sub> asymmetric and N–O stretches, respectively) for the solvated NO<sub>3</sub><sup>-</sup> molecule in the  $Cs^+$ ·(HNO<sub>3</sub>)(H<sub>2</sub>O)<sub>10</sub> cluster. The doublet peaks ( $\nu_{AAD}^{free}$  and  $\nu_{AD}^{free}$ ) in trace D denote water molecules in AAD and AD H-bonding sites. Remaining labels are described in Figure 1 caption. All band labels aid referencing in the text and in Tables S6, S8, and S9.

More complex band patterns are observed for the n = 4 and 5 clusters, displayed in panels B and G of Figure 2, respectively. Specifically, in addition to the features attributed to the ternary sandwich motif established in the smaller systems, they also display several new bands, suggesting the possibility that two or more isomers are in play. To address this possibility, we carried out isomer-selective, IR-IR photobleaching measurements with the results presented in Figure 2D,F. This method isolates the spectra of individual isomers in a mixture by setting a fixed frequency probe laser on a transition unique to one of the constituents and continuously monitoring the photofragment resulting from it, which in turn monitors the population of that species. The spectral pattern of a specific isomer is then obtained by exciting the same ion packet upstream from the probe laser with a second, powerful IR laser (the "bleach") that is scanned through the entire spectrum. The bleach laser depletes the population of all isomers as it drives the various transitions during the scan but only registers as depletions in the probe signal when transitions are common to both pump and probe frequencies.

Two distinct bleaching patterns were isolated for the n=4 cluster. One of these, corresponding to isomer 4I (structure

near Figure 2F), was revealed by setting the probe laser on the  $\nu_{\rm OH}^{\rm a-w}$  band (blue arrow in Figure 2F) and is similar to the patterns of the n=1-3 clusters (Figure 1B-D), indicating that a single water molecule is bound to OH<sup>a</sup>. That conclusion is supported by the calculated spectrum of the n=4 structure depicted in the inset and displayed by the lines in Figure 2E. The second pattern (assigned to isomer 4II) was recorded by setting the probe laser on the strong band at 3300 cm<sup>-1</sup> denoted  $\nu_{\rm AD}^{\rm bound}$  (orange arrow in Figure 2B). The spectrum of isomer 4II (structure in Figure 2B) displays a diffuse, redshifted envelope (highlighted orange near ~2300 cm<sup>-1</sup>) and slightly shifted bands in the region of the NO stretching and acidic OH bending fundamentals ( $v_{\rm NO}^{\rm a-2w}$  and  $v_{\rm bend}^{\rm a-2w}$ ). This basic pattern is also present in the  $v_{\rm a}$  spectrum and highlighted in orange in Figure 2G.

The spectral pattern of the 4II isomer is recovered at the (scaled) harmonic level (Figure 2C) by the calculated structure displayed in Figure 2B. Isomer 4II is calculated to lie 1.7 kcal/mol below the 4I structure displayed in Figure 2F and is also the lowest in energy identified in our survey of candidates. A sample of the various higher-energy isomers is included in Figure S3. The strong band at 3300 cm<sup>-1</sup> in the 4II

spectrum (Figure 2D) is traced to the interwater H-bond linking the water dimer that is attached to  $OH^a$  (hence denoted  $\nu_{AD}^{bound}$ ), while the red-shifted bands near 2300 cm<sup>-1</sup> occur near the harmonic prediction for the acidic OH stretch ( $\nu_{AD}^{a-2w}$ ).

Isomer 4II is interesting because its spectrum encodes the incremental structural deformation of the acid upon placing a water molecule in the second hydration shell relative to OHa. For example, this motif increases the OHa bond length by 0.017 Å on moving from n = 1 to n = 4, as the second water molecule acts to cooperatively enhance the H-bond to the adjacent water molecule. This stronger bond, in turn, blue shifts the OHa bending mode by 57 cm-1. As such, these spectra provide an excellent expression of the anticorrelation between the frequencies of the OHa stretch and its bending fundamental,<sup>33</sup> which is displayed in Figure S4. More subtle shifts are observed in the fingerprint region that appear as the close doublet patterns near 1400 cm<sup>-1</sup> assigned to the  $^{\text{sym}}\nu_{\text{NO}}^{\text{a-2w}}$ and  $\nu_{\rm bend}^{\rm a-2w}$  fundamentals in the nonselective spectrum (Figure 2B). The incremental structural displacements and associated shifts on the vibrational fundamentals are collected in Tables S3 and S4.

The spectral behaviors of the isomers at play in the n=4 and 5 clusters reveal how both the cation and the first and second shell water molecules act to partially displace the acidic proton toward the oxygen atom of the water directly bound to it. This raises the possibility that additional hydration can lead to a tipping point at which the proton is transferred to the water network in a cluster variation of acid dissolution. For example, such water-mediated charge separation has been reported to occur at surprisingly small sizes, indeed as small as n=4 in the  $HCl/(H_2O)_n$  system. Specifically, the lowest-energy n=4 structure corresponds to the solvent-separated ion pair  $[(HCl/(H_2O)_n \rightarrow H_3O^+(H_2O)_3Cl^-)]$  with the structure shown in Figure SSA. It features three water molecules bridging the  $H_3O^+$  and  $Cl^-$  charge centers in which each water adopts an acceptor—donor (AD) H-bonding configuration.

Figure 3 presents the D<sub>2</sub>-tagged vibrational spectra of the  $Cs^+ \cdot (HNO_3)(H_2O)_n \cdot D_2$  (n = 0, 7-11) clusters. The three bands assigned to the NO stretches of the intact HNO3 molecule bound to the Cs<sup>+</sup> ion are highlighted in purple in Figure 3A. The Cs<sup>+</sup>·(HNO<sub>3</sub>)(H<sub>2</sub>O), band patterns change dramatically from the open triplet pattern in the n = 7-9spectra before a simpler pattern emerges at n = 10. In particular, the doublet ( $\alpha$  and  $\beta$  in Figure 3E) near 1400 cm<sup>-1</sup>, in the vicinity of the NO stretches, is dramatically different from those in the spectrum of the intact acid. To establish the character of the bond displacements at play in these n = 10features, we measured their behaviors in the spectrum of the H<sup>15</sup>NO<sub>3</sub> isotopologue, with details included in Tables S5–S7 and Figures S6 and S7. The isotopic shifts allow us to unambiguously assign the doublet near 1400 cm<sup>-1</sup> in the n =10 to the NO stretching fundamentals. The difference in this band pattern from that of neutral HNO<sub>3</sub> (Figure 3A), signals a dramatic change in the structure of the NO<sub>3</sub> motif, providing a useful clue to the cause of the spectral complexity displayed by the n = 7-9 clusters. Such a change in the NO<sub>3</sub> scaffold is expected, for example, in the case where the acidic HNO<sub>3</sub> proton is transferred to the water network.

Because of the challenges involved in assigning structures to the n = 7-9 clusters based on their very diffuse spectra, we first focus on the likely structures that are responsible for the

simpler n = 10 band pattern. To this end, we first constrained candidate structures to meet the qualitative, empirical clues encoded in the spectrum. For example, the simple doublet in the region of the free OH stretching fundamentals ( $u_{
m AAD}^{
m free}$  and  $\nu_{\rm AD}^{\rm free}$  in Figure 3D) occurs in the tell-tale locations of water molecules in AAD and AD H-bonding sites (~3700 and 3720 cm<sup>-1</sup>) identified in many earlier studies.<sup>36–38</sup> This constraint allows the search to be focused on structures with roughly equal numbers of AAD and AD sites. Furthermore, it allows us to rule out structures that include water molecules in a single H-bond acceptor site, as this motif would result in the sharp  $\nu_{\rm A}^{\rm sym}$  and  $\nu_{\rm A}^{\rm asym}$  transitions (Figure 1B) that do not appear in the n = 10 spectrum. In particular, we can eliminate all of the lowlying minimum-energy structures that start with variations of the motifs present in the n = 2-6 clusters (their minimumenergy structures and associated calculated spectra are included in Figures S1 and S2). An important additional clue is the appearance of a prominent band centered at ~2600 cm<sup>-1</sup>, which is known to occur when the excess proton is localized on a 3-fold coordinated hydronium ion, like in the H<sub>3</sub>O<sup>+</sup>(H<sub>2</sub>O)<sub>3</sub>, so-called Eigen cation.<sup>39,40</sup> The characteristic OH hydronium stretch in the Eigen cation at 2646 cm<sup>-1</sup> is indicated by the arrow labeled  $\nu_{\mathrm{H_3O^+}}$  in Figure 3E. After an extensive search (Figure S8), we identified the global minimum structure depicted in Figure 4 that meets all these spectroscopic requirements as evidenced by the comparison with its calculated (scaled) harmonic spectrum in Figure 4B.

The structure in Figure 4 is compelling because it exhibits a variation in bonding motif that is adopted in the dissociation of HCl and HBr in small water clusters as shown in Figure S5B. 41,42 In particular, the three water molecules attached to the hydronium ion occur in AD configuration, two of which form a bridge to the two oxygen atoms of the NO<sub>3</sub><sup>-</sup> anion. The coordination environment of the Cs<sup>+</sup> ion is also compelling in that NO<sub>2</sub> binds to the Cs<sup>+</sup> ion in a bidentate fashion, similar to the arrangement in the smaller clusters, while the water network near the cation occurs in a distorted "book" form of the water hexamer. 43 Two of the "corner" water molecules on the book dock onto the solvent-separated ion-pair (SSIP): one to the remaining O atom of  $NO_3^-$  and the other to the third AD water molecule bound to  $H_3O^+$ . Overall, this n=10 isomer can be regarded as a microhydrated Cs<sup>+</sup>-NO<sub>3</sub><sup>-</sup>-H<sub>3</sub>O<sup>+</sup> saltbridge motif in which the Cs+ cation binds directly to the NO<sub>3</sub><sup>-</sup> anion that, in turn, forms a solvent-separated ion-pair with the hydronium cation.

The assignment of the n = 10 cluster structure to the saltbridge motif also provides context for the spectral complexity displayed by the n = 7-9 clusters (Figure 3B–D). In particular, these more diffuse band patterns can be readily explained by the large changes in the water network expected to occur in the size range where charge separation begins to occur. For example, it is likely that many different isomers will be in play before the NO<sub>3</sub><sup>-</sup> and H<sub>3</sub>O<sup>+</sup> charge-localized ions are fully coordinated in the n = 10 structure. We note that the n = 107 and 8 spectra both display an intense, diffuse band near 1000 cm<sup>-1</sup>, which is close to the parallel stretch of the bridging proton stretch in systems where the excess proton is equally shared in the O-H+-O class of proton-bound molecules  $(\nu_{O-H-O})$  red arrow in Figure 3C). We therefore speculate that this absorption in the n = 8 spectrum signals the formation of structures in which the acidic proton is close to the tipping point for intermolecular proton transfer.<sup>27</sup> The n = 9 case is

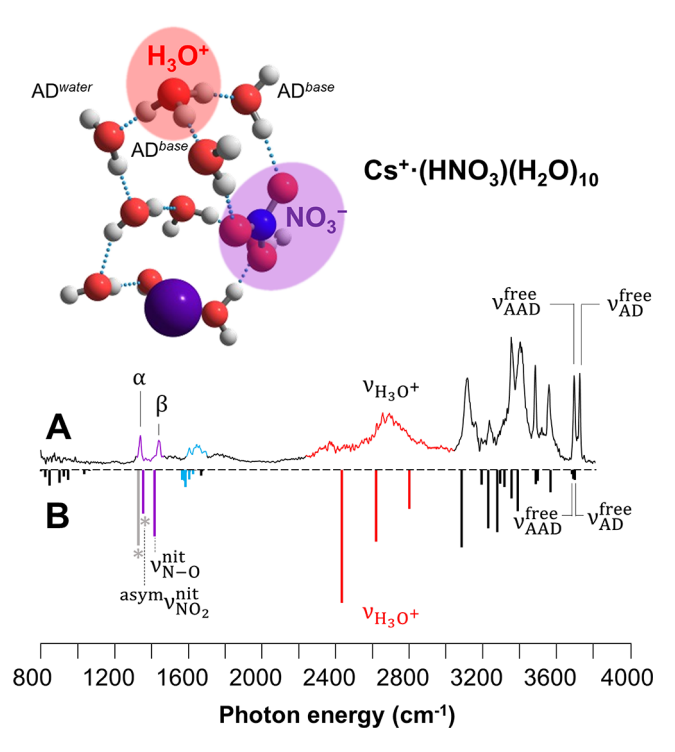


**Figure 4.** (A) Vibrational predissociation spectrum of Cs<sup>+</sup>·(HNO<sub>3</sub>)-(H<sub>2</sub>O)<sub>10</sub>·D<sub>2</sub>. (B) Calculated (inverted) spectrum of proposed minimum-energy structure (inset) for Cs<sup>+</sup>·(HNO<sub>3</sub>)(H<sub>2</sub>O)<sub>10</sub> at B3LYP/(H,O,N: aug-cc-pVDZ, Cs: LANL2DZ) level of theory and basis set, scaled by a factor of 0.9576 in 2200–4000 cm<sup>-1</sup> range and 0.9719 in 800–2200 cm<sup>-1</sup> range. The calculated peaks marked with \* are both a mixture of two bands, with the predominant motions for each frequency being H<sub>3</sub>O<sup>+</sup> umbrella mode (gray peak) and  $^{\rm asym}\nu_{\rm NO_2}^{\rm nit}$  for NO<sub>3</sub><sup>-</sup> (purple peak). Remaining labels are described in Figure 3 caption.

particularly interesting in that it displays a series of sharp bands in the NO stretching region near 1300–1400 cm<sup>-1</sup> ( $\alpha' - \epsilon'$  in Figure 3D) that occur in the vicinity of the strong doublet ( $\alpha$ and  $\beta$  in Figure 3E) traced to the NO stretches of the NO<sub>3</sub> anion in the n = 10 spectrum. This behavior suggests that the n= 8 and 9 clusters occur in several different isomeric forms that yield different degrees of proton transfer, each with a distinct pair of NO stretching fundamentals along with the OH stretching bands arising from the partial transfer of the acidic proton. The contributions from the latter thus rationalize the extreme breadth of the n = 9 features in the OH stretching region between 2000 and 3000 cm<sup>-1</sup>, none of which are expected for water molecules involved in a neutral network. The contributions of these putative isomers can be isolated as was carried out for the n = 4 and 5 clusters, but this lies beyond the scope of this report outlining the general observation of ion-mediated charge separation. We note that in the n=11spectrum (Figure 3F), the NO stretches again appear as multiplets, suggesting that many isomers are again in play. This behavior implies that n = 10 occurs as a "magic number" in that it adopts a particularly stable arrangement that effectively locks the three ions in place.

This observation of size-dependent charge separation raises many interesting questions, such as whether the SSIP motif is retained in the cold clusters with increasing cluster size and whether the SSIP structures can be accessed in the smaller clusters at elevated temperature. Another important issue concerns the role of the electric field from the Cs<sup>+</sup> cation in

driving the tipping point for charge separation. This can be addressed by extending the study to other alkali metal ions as well as the halide ions to vary the ionic radius and thus the strength and sign of the local electric field in the vicinity of the acid. All of these results will provide unambiguous experimental benchmarks for ongoing theoretical work directed toward simulating the chemistry of complex water interfaces at the molecular level.

We have reported how the strong acid HNO<sub>3</sub> responds to the incremental addition of water molecules to the Cs+.HNO<sub>3</sub> binary ion cluster. Two isomeric classes are observed in the n =1-6 size range, one of which features a single water molecule attached to the acidic OH group, while the other occurs with attachment of a water dimer. Addition of the second water yields an additional ~360 cm<sup>-1</sup> red shift in the acidic OH stretch along with smaller shifts in the NO stretching fundamentals that signal partial deformation of the NO<sub>3</sub> scaffold toward that of the NO<sub>3</sub><sup>-</sup> conjugate base. Although very complex and diffuse spectra are observed in the n = 7-9range, the n = 10 cluster spectrum is again simple and is assigned to a new charge accommodation motif involving formation of a Cs<sup>+</sup>-NO<sub>3</sub><sup>-</sup>-H<sub>3</sub>O<sup>+</sup> salt bridge. In this structure, the latter two ions adopt a solvent-separated ion pair configuration in which H<sub>3</sub>O<sup>+</sup> is surrounded by three water molecules in AD network sites. These results thus reveal the highly cooperative intermolecular interactions at play in ionassisted acid dissociation at the molecular level.

### ASSOCIATED CONTENT

#### Supporting Information

The Supporting Information is available free of charge at https://pubs.acs.org/doi/10.1021/acs.jpclett.1c00235.

Experimental and computational methods, tables for experimental and calculated frequencies, computed minimum-energy structures and associated spectra compared with experimental spectra, acid OH stretch and bend frequencies analyzed with respect to bond lengths, and the mass spectrum of acid uptake on clusters (PDF)

# AUTHOR INFORMATION

#### **Corresponding Author**

Mark A. Johnson — Sterling Chemistry Laboratory, Yale University, New Haven, Connecticut 06511, United States; orcid.org/0000-0002-1492-6993; Email: mark.johnson@yale.edu

#### Authors

Sayoni Mitra — Sterling Chemistry Laboratory, Yale University, New Haven, Connecticut 06511, United States; orcid.org/0000-0003-4526-730X

Nan Yang — Sterling Chemistry Laboratory, Yale University, New Haven, Connecticut 06511, United States; orcid.org/ 0000-0003-1253-2154

Laura M. McCaslin — Combustion Research Facility, Sandia National Laboratories, Livermore, California 94550, United States; © orcid.org/0000-0002-6705-8755

R. Benny Gerber — Institute of Chemistry and the Fritz-Haber Center for Molecular Dynamics, The Hebrew University, Jerusalem, Israel; Department of Chemistry, University of California Irvine, Irvine, California 92697, United States; orcid.org/0000-0001-8468-0258 Complete contact information is available at: https://pubs.acs.org/10.1021/acs.jpclett.1c00235

#### Notes

The authors declare no competing financial interest.

#### ACKNOWLEDGMENTS

M.A.J. thanks the NSF Center for Aerosol Impacts on Chemistry of the Environment (CAICE) for support of this work (CHE-1801971). N.Y. was supported by the U.S. Department of Energy grant DE-FG02-06ER15800 continued under DE-SC0021012. We thank Dr. Chinh Duong for his valuable assistance in acquiring the early data for this system. The work presented here by L.M.M. is supported by the Division of Chemical Sciences, Geosciences and Biosciences, Office of Basic Energy Sciences (BES), U.S. Department of Energy (USDOE). Sandia National Laboratories is a multimission laboratory managed and operated by National Technology and Engineering Solutions of Sandia, LLC., a wholly owned subsidiary of Honeywell International, Inc., for the U.S. Department of Energy's National Nuclear Security Administration under contract DE-NA-0003525. This paper describes objective technical results and analysis. Any subjective views or opinions that might be expressed in the paper do not necessarily represent the views of the U.S. Department of Energy or the United States Government.

# REFERENCES

- (1) Abbatt, J. P. D. Interaction of HNO<sub>3</sub> with Water-Ice Surfaces at Temperatures of the Free Troposphere. *Geophys. Res. Lett.* **1997**, 24 (12), 1479-1482.
- (2) Zondlo, M. A.; Barone, S. B.; Tolbert, M. A. Uptake of HNO<sub>3</sub> on Ice under Upper Tropospheric Conditions. *Geophys. Res. Lett.* **1997**, 24 (11), 1391–1394.
- (3) Rivera-Figueroa, A. M.; Sumner, A. L.; Finlayson-Pitts, B. J. Laboratory Studies of Potential Mechanisms of Renoxification of Tropospheric Nitric Acid. *Environ. Sci. Technol.* **2003**, 37 (3), 548–554.
- (4) Guimbaud, C.; Arens, F.; Gutzwiller, L.; Gaggeler, H. W.; Ammann, M. Uptake of HNO<sub>3</sub> to Deliquescent Sea-Salt Particles: A Study using the Short-Lived Radioactive Isotope Tracer N-13. *Atmos. Atmos. Chem. Phys.* **2002**, *2*, 249–257.
- (5) Lawrence, M. G.; Crutzen, P. J. The Impact of Cloud Particle Gravitational Settling on Soluble Trace Gas Distributions. *Tellus, Ser. B* **1998**, *50* (3), 263–289.
- (6) Zondlo, M. A.; Hudson, P. K.; Prenni, A. J.; Tolbert, M. A. Chemistry and Microphysics of Polar Stratospheric Clouds and Cirrus Clouds. *Annu. Rev. Phys. Chem.* **2000**, *51*, 473–499.
- (7) Hudson, P. K.; Shilling, J. E.; Tolbert, M. A.; Toon, O. B. Uptake of nitric acid on ice at tropospheric temperatures: Implications for cirrus clouds. *J. Phys. Chem. A* **2002**, *106* (42), 9874–9882.
- (8) Kuo, M. H.; David, A.; Kamelamela, N.; White, M.; Shultz, M. J. Nitric acid Water Interaction Probed via Isolation in Carbon Tetrachloride. *J. Phys. Chem. C* **2007**, *111* (25), 8827–8831.
- (9) Kido Soule, M. C.; Blower, P. G.; Richmond, G. L. Nonlinear Vibrational Spectroscopic Studies of the Adsorption and Speciation of Nitric Acid at the Vapor/Acid Solution Interface. *J. Phys. Chem. A* **2007**, *111* (17), 3349–3357.
- (10) Shamay, E. S.; Buch, V.; Parrinello, M.; Richmond, G. L. At the Water's Edge: Nitric Acid as a Weak Acid. *J. Am. Chem. Soc.* **2007**, 129 (43), 12910–12911.
- (11) Wang, S. Z.; Bianco, R.; Hynes, J. T. Depth-Dependent Dissociation of Nitric Acid at an Aqueous Surface: Car-Parrinello Molecular Dynamics. *J. Phys. Chem. A* **2009**, *113* (7), 1295–1307.
- (12) Baer, M. D.; Kuo, I. F. W.; Tobias, D. J.; Mundy, C. J. Toward a Unified Picture of the Water Self-Ions at the Air—Water Interface: A

- Density Functional Theory Perspective. J. Phys. Chem. B 2014, 118 (28), 8364-8372.
- (13) Wang, S. Z.; Bianco, R.; Hynes, J. T. An Atmospherically Relevant Acid: HNO<sub>3</sub>. Comput. Theor. Chem. **2011**, 965 (2–3), 340–345
- (14) Lewis, T.; Winter, B.; Stern, A. C.; Baer, M. D.; Mundy, C. J.; Tobias, D. J.; Hemminger, J. C. Does Nitric Acid Dissociate at the Aqueous Solution Surface? *J. Phys. Chem. C* **2011**, *115* (43), 21183–21190.
- (15) Wren, S. N.; Donaldson, D. J. Glancing-Angle Raman Study of Nitrate and Nitric Acid at the Air-Aqueous interface. *Chem. Phys. Lett.* **2012**, *522*, 1–10.
- (16) Riikonen, S.; Parkkinen, P.; Halonen, L.; Gerber, R. B. Ionization of Nitric Acid on Crystalline Ice: The Role of Defects and Collective Proton Movement. *J. Phys. Chem. Lett.* **2013**, 4 (11), 1850–1855.
- (17) Otten, D. E.; Shaffer, P. R.; Geissler, P. L.; Saykally, R. J. Elucidating the Mechanism of Selective Ion Adsorption to the Liquid Water Surface. *Proc. Natl. Acad. Sci. U. S. A.* **2012**, *109* (3), 701–705.
- (18) Knipping, E. M.; Lakin, M. J.; Foster, K. L.; Jungwirth, P.; Tobias, D. J.; Gerber, R. B. Experiments and Simulations of Ion-Enhanced Interfacial Chemistry on Aqueous NaCl aerosols. *Science* **2000**, 288, 301–306.
- (19) Jungwirth, P.; Tobias, D. J. Ions at the Air/Water interface. *J. Phys. Chem. B* **2002**, *106*, 6361–6373.
- (20) Tobias, D. J.; Stern, A. C.; Baer, M. D.; Levin, Y.; Mundy, C. J. Simulation and Theory of Ions at Atmospherically Relevant Aqueous Liquid-Air Interfaces. *Annu. Rev. Phys. Chem.* **2013**, *64*, 339–359.
- (21) Marchand, P.; Marcotte, G.; Ayotte, P. Spectroscopic Study of HNO3 Dissociation on Ice. *J. Phys. Chem. A* **2012**, *116* (49), 12112–12122.
- (22) Mishra, H.; Nielsen, R. J.; Enami, S.; Hoffmann, M. R.; Colussi, A. J.; Goddard, W. A., III Quantum Chemical Insights into the Dissociation of Nitric Acid on the Surface of Aqueous Electrolytes. *Int. J. Quantum Chem.* **2013**, *113* (4), 413–417.
- (23) Gilligan, J. J.; Castleman, A. W. Acid Dissolution by Aqueous Surfaces and Ice: Insights from a Study of Water Cluster Ions. *J. Phys. Chem. A* **2001**, *105* (23), 5601–5605.
- (24) Wolk, A. B.; Leavitt, C. M.; Garand, E.; Johnson, M. A. Cryogenic Ion Chemistry and Spectroscopy. *Acc. Chem. Res.* **2014**, 47 (1), 202–210.
- (25) Mitra, S.; Duong, C. H.; McCaslin, L. M.; Gerber, R. B.; Johnson, M. A. Isomer-Specific Cryogenic Ion Vibrational Spectroscopy of the  $D_2$ -Tagged  $Cs^+(HNO_3)(H_2O)_{(n=0-2)}$  Complexes: Ion-Driven Enhancement of the Acidic H-Bond to Water. *Phys. Chem. Chem. Phys.* **2020**, 22 (8), 4501–4507.
- (26) Canagaratna, M.; Phillips, J. A.; Ott, M. E.; Leopold, K. R. The Nitric Acid-Water Complex: Microwave Spectrum, Structure, and Tunneling. J. Phys. Chem. A 1998, 102 (9), 1489–1497.
- (27) Wolke, C. T.; Fournier, J. A.; Dzugan, L. C.; Fagiani, M. R.; Odbadrakh, T. T.; Knorke, H.; Jordan, K. D.; McCoy, A. B.; Asmis, K. R.; Johnson, M. A. Spectroscopic Snapshots of the Proton-Transfer Mechanism in Water. *Science* **2016**, *354* (6316), 1131–1135.
- (28) Relph, R. A.; Guasco, T. L.; Elliott, B. M.; Kamrath, M. Z.; McCoy, A. B.; Steele, R. P.; Schofield, D. P.; Jordan, K. D.; Viggiano, A. A.; Ferguson, E. E.; et al. How the Shape of an H-Bonded Network Controls Proton-Coupled Water Activation in HONO Formation. *Science* 2010, 327, 308–312.
- (29) Ali, S. M.; De, S.; Maity, D. K. Microhydration of  $Cs^+$  ion: A Density Functional Theory Study on  $Cs^+(H_2O)_{(n)}$  clusters (n = 1–10). *J. Chem. Phys.* **2007**, *127* (4), No. 044303.
- (30) Miller, D. J.; Lisy, J. M. Hydrated Alkali-Metal Cations: Infrared Spectroscopy and ab Initio Calculations of  $M^+(H_2O)_{x=2-5}$  Ar cluster ions for M = Li, Na, K, and Cs. J. Am. Chem. Soc. **2008**, 130 (46), 15381–15392.
- (31) Miller, D. J.; Lisy, J. M. Entropic Effects on Hydrated Alkali-Metal Cations: Infrared Spectroscopy and ab Initio Calculations of  $M^+(H_2O)_{x=2-5}$  Cluster Ions for M = Li, Na, K, and Cs. J. Am. Chem. Soc. **2008**, 130 (46), 15393–15404.

- (32) Denton, J. K.; Kelleher, P. J.; Johnson, M. A.; Baer, M. D.; Kathmann, S. M.; Mundy, C. J.; Wellen Rudd, B. A.; Allen, H. C.; Choi, T.; Jordan, K. D. Molecular-level Origin of the Carboxylate Head Group Response to Divalent Metal Ion Complexation at the Air-Water Interface. *Proc. Natl. Acad. Sci. U. S. A.* **2019**, *116* (30), 14874–14880.
- (33) Seki, T.; Chiang, K. Y.; Yu, C. C.; Yu, X. Q.; Okuno, M.; Hunger, J.; Nagata, Y.; Bonn, M. The Bending Mode of Water: A Powerful Probe for Hydrogen Bond Structure of Aqueous Systems. *J. Phys. Chem. Lett.* **2020**, *11* (19), 8459–8469.
- (34) Gutberlet, A.; Schwaab, G.; Birer, O.; Masia, M.; Kaczmarek, A.; Forbert, H.; Havenith, M.; Marx, D. Aggregation-Induced Dissociation of  $HCl(H_2O)_4$  Below 1 K: The Smallest Droplet of Acid. Science **2009**, 324 (5934), 1545–1548.
- (35) Milet, A.; Struniewicz, C.; Moszynski, R.; Wormer, P. E. S. Theoretical Study of the Protolytic Dissociation of HCl in Water Clusters. *J. Chem. Phys.* **2001**, *115* (1), 349–356.
- (36) Yang, N.; Duong, C. H.; Kelleher, P. J.; McCoy, A. B.; Johnson, M. A. Deconstructing Water's Diffuse OH Stretching Vibrational Spectrum With Cold Clusters. *Science* **2019**, 364 (6437), 275–278.
- (37) Fournier, J. A.; Wolke, C. T.; Johnson, M. A.; Odbadrakh, T. T.; Jordan, K. D.; Kathmann, S. M.; Xantheas, S. S. Snapshots of Proton Accommodation at a Microscopic Water Surface: Understanding the Vibrational Spectral Signatures of the Charge Defect in Cryogenically Cooled  $H^+(H_2O)_{n=2-28}$  clusters. J. Phys. Chem. A 2015, 119 (36), 9425–9440.
- (38) Miyazaki, M.; Fujii, A.; Ebata, T.; Mikami, N. Infrared Spectroscopic Evidence for Protonated Water Clusters Forming Nanoscale Cages. *Science* **2004**, *304*, 1134–1137.
- (39) Okumura, M.; Yeh, L. I.; Myers, J. D.; Lee, Y. T. Infrared-Spectra of the Solvated Hydronium Ion: Vibrational Predissociation Spectroscopy of Mass-Selected  $H_3O^+\cdot (H_2O)_n\cdot (H_2)_m$ . *J. Phys. Chem.* **1990**, *94*, 3416–3427.
- (40) Duong, C. H.; Yang, N.; Kelleher, P. J.; Johnson, M. A.; DiRisio, R. J.; McCoy, A. B.; Yu, Q.; Bowman, J. M.; Henderson, B. V.; Jordan, K. D. Tag-free and Isotopomer-Selective Vibrational Spectroscopy of the Cryogenically Cooled H<sub>9</sub>O<sub>4</sub><sup>+</sup> Cation with Two-Color, IR-IR Double-Resonance Photoexcitation: Isolating the Spectral Signature of a Single OH group in the Hydronium Ion Core. *J. Phys. Chem. A* **2018**, *122* (48), 9275–9284.
- (41) Gertner, B. J.; Peslherbe, G. H.; Hynes, J. T. Acid Ionization of HBr in a Small Water Cluster. *Isr. J. Chem.* **1999**, *39*, 273–281.
- (42) Robertson, W. H.; Johnson, M. A. Caught in the Act of Dissolution. *Science* **2002**, 298, 69.
- (43) Perez, C.; Muckle, M. T.; Zaleski, D. P.; Seifert, N. A.; Temelso, B.; Shields, G. C.; Kisiel, Z.; Pate, B. H. Structures of Cage, Prism, and Book Isomers of Water Hexamer from Broadband Rotational Spectroscopy. *Science* **2012**, *336* (6083), 897–901.
- (44) Mcgraw, G. E.; Bernitt, D. L.; Hisatsune, I. C. Vibrational Spectra of Isotopic Nitric Acids. J. Chem. Phys. 1965, 42 (1), 237.